ISSN 1526-5757

# 49. A possible unsuspected significance of isotopic Rb-Sr "errorchrons"

**Lorence G. Collins and Barbara J. Collins**

**April 29, 2004**

lorencecollins@gmail.com

## ABSTRACT

Rb-Sr isotopic data that produce "errorchrons" with large ± error values are commonly not published because more accurate dates calculated from isochrons are sought. An assumption is generally made that Sr is the only element that has moved out of the system when an errorchron is produced, but little work has been done to verify this hypothesis. A Rb-Sr errorchron occurs when data are plotted from chemically analyzed samples collected in the Kernville diorite-gabbro, north of the Lake Isabella Reservoir in the southern Sierra Nevada. Detailed structural, mineralogical, chemical, and Rb-Sr isotopic examinations of aplite-pegmatite-migmatite dikes and their transitions to Kernville diorite north of Lake, show how data that produce a Rb-Sr errorchron are generated. The changes in mineralogy and whole-rock major- and trace-element compositions in the modified transition rocks reveal different movements of both Rb and Sr isotopes as well as other trace elements and major oxides. On that basis, other terranes producing Rb-Sr isotopic data that plot as an errorchron should be examined carefully to see if major changes in mineralogy and chemistry are associated with processes that created the errorchron.

## Introduction

When age-daters use Rb and Sr isotopic data to estimate ages of granitic rocks, the analyzed data obtained for some rocks are sufficiently scattered that the data do not all fall on a straight isochron line. When that occurs, an "errorchron" is produced instead of an isochron, and such an errorchron indicates an age whose +/- error values are too large to be acceptable. Therefore, these Rb-Sr data generally are never published when rock ages are sought. Petrologists commonly claim that in such places, the rocks have been subjected to an open system in which soluble Sr has been unequally removed from different places by through-going fluids, thereby disrupting the Rb-Sr systematics. It is illogical, however, that these fluids are specifically selective to remove only Sr. On that basis, the scattered Rb-Sr isotopic data that fall off isochrons could well be a clue to unrecognized movements of other trace elements as well as major elements. In the following sections, structural, mineralogical, chemical, and Rb-Sr isotopic data, published previously (Collins, 1988, 1989; Hunt et al., 1992), are used to demonstrate how an open system was created in the diorite-gabbro Kernville pluton in the southern Sierra Nevada which allowed differential movements of Rb and Sr isotopes that produced a Rb-Sr errorchron.

**Geologic situation**

A small quartz diorite and gabbro mass (hereafter called diorite-gabbro) lies 8 km northeast of Isabella, California (Fig. 1), north of Lake Isabella Reservoir (Fig. 2). This mass forms the western wall rock of the Isabella pluton in the southern Sierra Nevada, and the gabbro portion of this mass occurs mostly at and near the western border. The Proto-Kern Canyon-Sierra Crest Fault zone (Saleeby, 2003) extends northward, just west of the diorite-gabbro, through the valley containing the Kern River (Fig. 1). Movements along this fault zone likely produced the deformation that occurs in the diorite-gabbro. Kistler (written communication, 1983) dated the diorite-gabbro (the Kernville pluton) by Rb-Sr isotopic methods as being 120.1 million years old. The oldest rocks bordering the pluton are Paleozoic (?) Kernville metasediments (Fig. 1), consisting of weakly metamorphosed phyllites, mica schists, marbles, and quartzites (Miller, 1931; Miller and Webb, 1940; Elan, 1985).

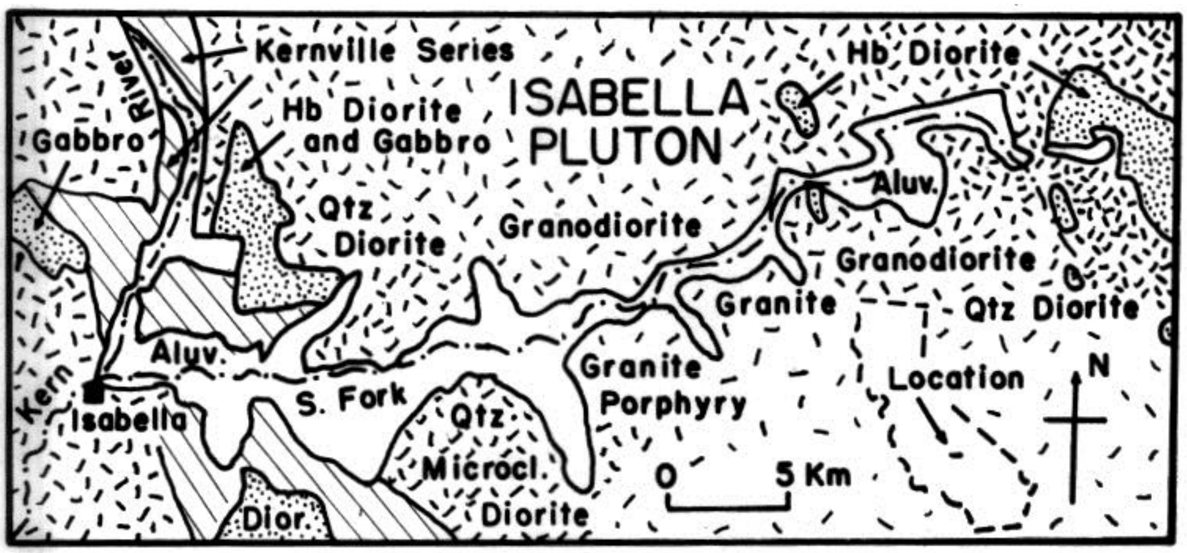


**Fig. 1.** Geologic map of the Isabella pluton, showing location of hornblende (HB) diorite and gabbro wall rock (Kernville pluton) and the Kernville metasedimentary series: see text. Modified after Miller (1931) and Miller and Webb (1940), keeping their generalized map pattern but emphasizing locations of different rock facies. The Proto-Kern Canyon-Sierra Crest fault zone extends northward in the Kern River valley west of the small diorite and gabbro pluton.

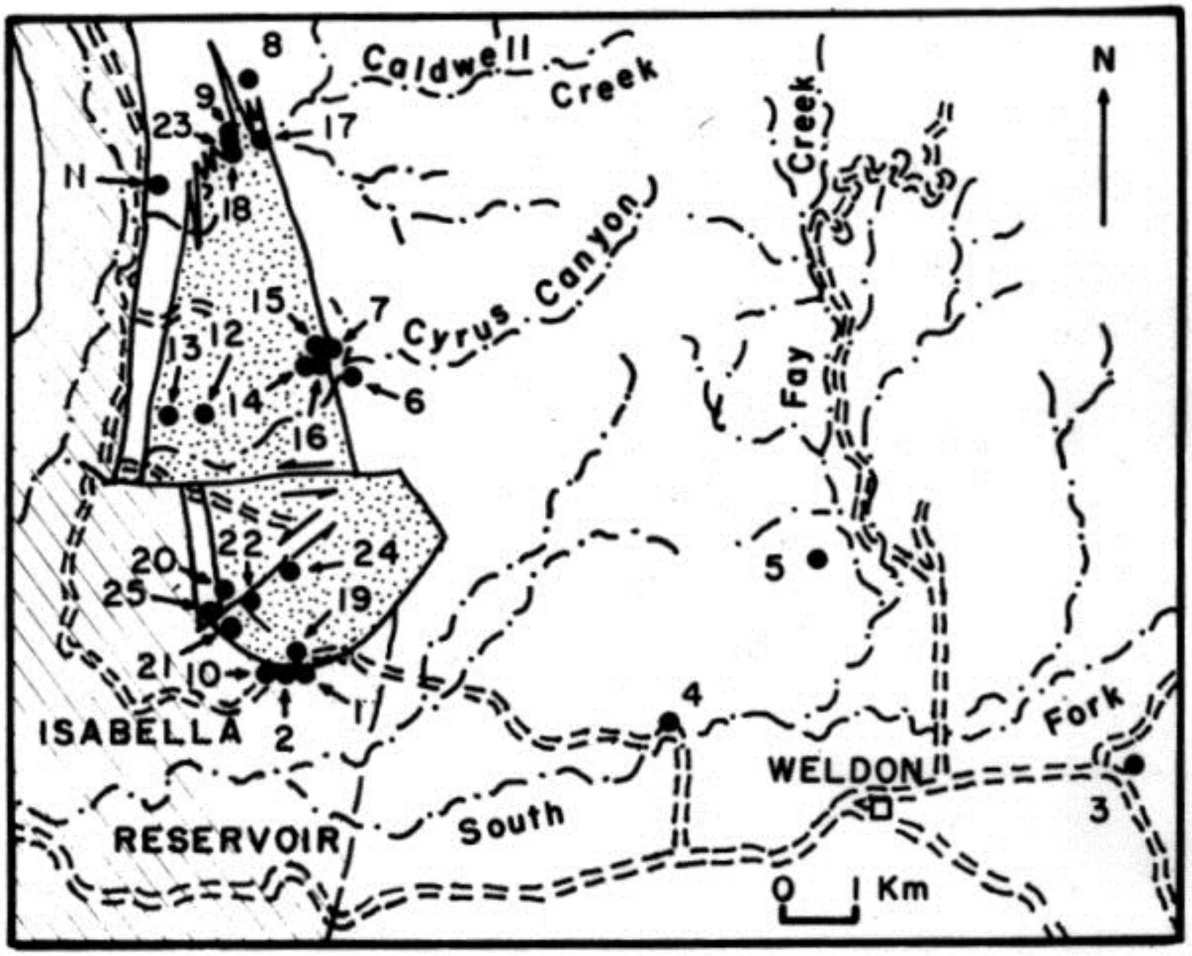


**Fig. 2.** Location map of chemically analyzed samples listed in Tables VI and VII in Collins (1988), but not discussed in this article. Slanted line area = Kernville metasedimentary series: dot pattern = diorite-gabbro of the Kernville pluton; unshaded = Isabella pluton. Outline of the Isabella Reservoir is not shown - only the general position.

Miller and Webb (1940) mapped the diorite-gabbro as an irregular L-shaped body, about 10 km long and 3.5 km wide, with a broad base at the south against Kernville metasedimentary rocks (Fig. 1). When mapped in more detail, however, the diorite-gabbro appears as an elongate, faulted body (Fig. 2). At its northern edge it tapers to an irregular jagged point where many hundreds of north-south to north-15-degrees-west-trending aplite-pegmatite dikes extend as fingers into the diorite-gabbro, seemingly from the Isabella pluton. All of these dikes are not shown in Fig. 2, except schematically, because of the small scale of the map. Southward, the dikes disappear progressively until only fifteen to twenty cut the diorite-gabbro mass on the north side of Cyrus Canyon (Fig. 2). Here, the dikes range from 10-cm-wide migmatitic zones to 5-m-wide migmatite-aplite-pegmatite zones that trend north-south to north-15-degrees-east. South of Cyrus Canyon, only two or three dikes remain, and these disappear before the southern contact with the Paleozoic metasediments is reached.

**Magmatic intrusions or replacements in an open system**

The granitic dikes appear to represent extensions of the Isabella pluton (Fig. 1 and Fig. 2), intruding as magma into cracks and fractures in the northern part of the older diorite-gabbro. Crosscutting relationships in a few places, sharp contacts, and contrasting mineral and chemical compositions between the two rock types seem to imply a magmatic origin. However, if the dikes extending from the Isabella pluton were intrusive in cracks in the diorite-gabbro, then the many hundreds of granitic dikes should have spread apart the tapered apex of the diorite-gabbro because of the added volume of rock in the cracks. If that occurred, the diorite-gabbro would have opened up like a spreading fan (Fig. 3, A), just as pushing matter between one's fingers will spread the fingers apart. The absence of any dilation from west to east across the northern part of the diorite-gabbro mass suggests that intrusion of magma may not have occurred, but instead, the granitic dikes were formed by differential movements and losses of some whole-rock major- and trace-elements in an open system in microfractured solidified diorite-gabbro, and the losses caused shrinkage to occur (Fig. 3, B). Among the trace elements that moved differentially are Rb and Sr isotopes. To determine what caused these isotopes to move differentially, changes in fabric, mineralogy, structure, and chemistry are examined in detail in one of these former open systems - an aplite-pegmatite dike and its wall rocks on the north side of Cyrus Canyon (Fig. 2).

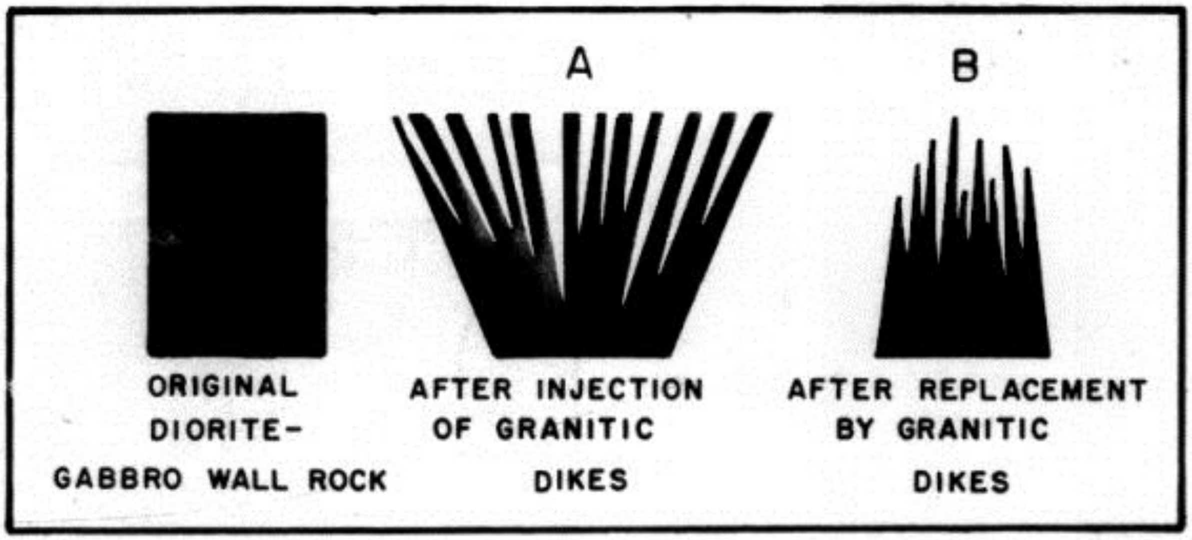


**Fig. 3.** Diagram to show (A) the effects of physical injection of magma to form granitic dikes versus (B) the effects of volume-for-volume replacements to form granitic dikes.

**Fabric changes.**

As portrayed on Fig. 4, the dike stands out as a wall because of its greater resistance to erosion. On the east (right) side, 10 m from the dike, the diorite appears to be massive, lacking any deformation (schematically shown on Fig. 4 as zone 0). However, toward the dike, deformation increases in intensity and causes a foliation to appear (Fig. 4, zone 1). Greater degrees of cataclasis occur progressively toward the dike, producing broken grains, mortar texture, and a foliation. Farthest from the dike the foliation is inclined to the strike of the dike, but near the dike the inclination gradually becomes nearly parallel to the dike. Where the foliation becomes parallel, the rock becomes migmatitic (Fig. 4, zone 2). Finally, in the center of the dike, aplite and pegmatite occur. Note that on the west (left) side of the dike, the inclined foliated rock (Fig. 4, zone 1) is schematically shown to be less than a meter thick. Such a narrower relationship occurs in some places, but in other places, the width of zone 1 is about the same on both sides and commonly is as much as 30 m wide. Generally, the wider or more strongly deformed zone 1 is, the thicker is the associated dike.

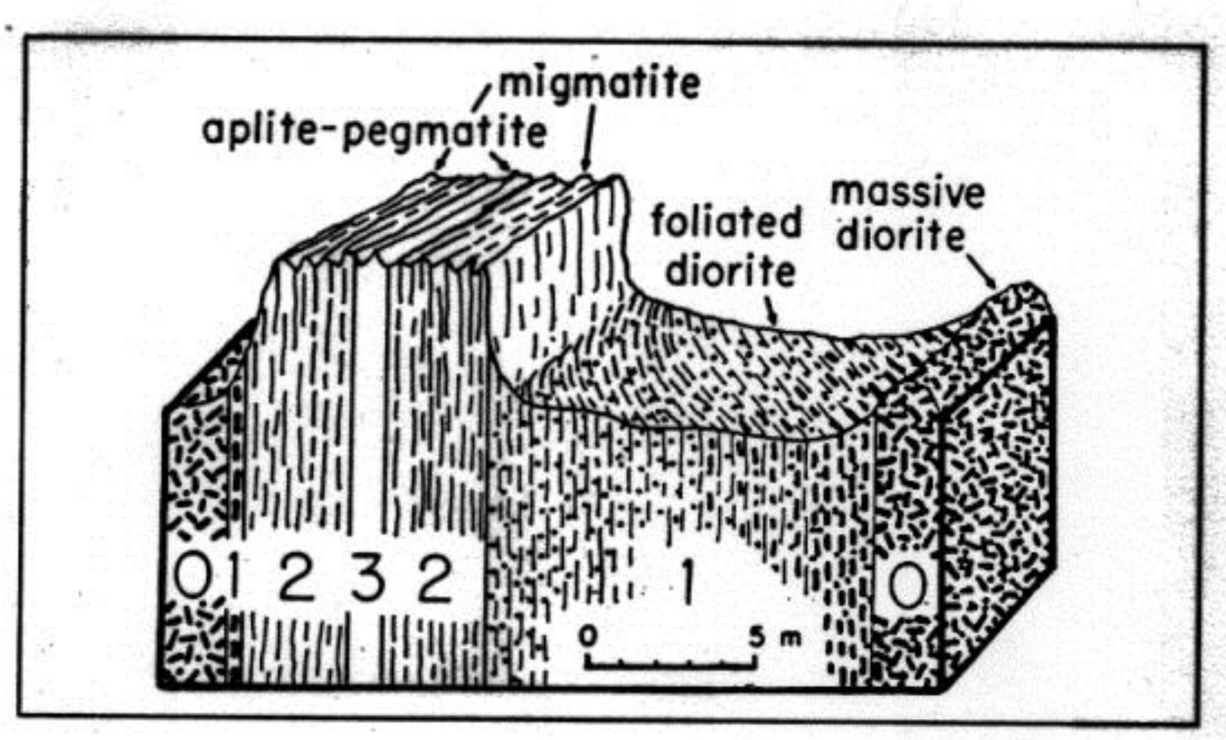


**Fig. 4.** Schematic diagram for mode of formation of migmatite and aplite-pegmatite dikes in the Kernville diorite-gabbro pluton, southern Sierra Nevada, California. Zone 0 = massive diorite; zone 1 = transition rocks; zone 2 = migmatite; zone 3 = aplite-pegmatite.

**Mineralogical changes.**

Across the eastern interval from zone 0 to zone 3 (Fig. 4), the following mineralogical changes were observed in thin sections as the structural attitudes in the rocks changed. In zone 0, plagioclase (43-68%), hornblende (5-32%), biotite (12-20%), and quartz (8-13%) are undisturbed, exhibiting normal, randomly oriented, unmodified, igneous textures. But in the transition (zone 1), plagioclase exhibits bent albite-twin lamellae, and hornblende and biotite contain occasional small quartz blebs. In more strongly sheared and replaced rocks toward zone 2, the hornblende disappears as quartz increases in abundance. Farther across the transition, biotite shows a progressive replacement by quartz, but biotite does not disappear as rapidly as hornblende, and some biotite generally remains in the granitic residue. In early stages of replacement the plagioclase grains may retain their oscillatory zoning with calcic cores, but in and near the granitic aplite dikes, they recrystallize as unzoned more-sodic crystals. The An content is reduced from higher values ($An_{38-52}$) in diorite to lower values ($An_{18-35}$) in the dikes. Midway across zone 1, microcline replaces cores of some microfractured plagioclase grains and then completely replaces other plagioclase grains. As the microcline becomes more abundant, wartlike myrmekite also appears. These progressive recrystallization and replacements heal much of the cataclasis and change the mineralogy into granitic end-products in zone 2 that look like feldspathic quartzites and mafic well-foliated metasediments in migmatite. Finally, a central aplite-pegmatite is created in zone 3 (Fig. 4). Here, the replaced and recrystallized former diorite, now aplite-pegmatite, contains quartz (10-35%), microcline (20-40%), recrystallized, more-sodic, unzoned plagioclase (30-55%), and biotite (0-5%).

**Structural changes.**

A schematic diagram (Fig. 5) shows how three stages in an S-shaped structure produce an open system in which the rock composition can change. Movements of the foliated rocks (sliding in opposite directions on either side of an S-shaped flexure) created central low-pressure sites. These sites are places where hydrous fluids carrying major- and trace-elements could migrate. The greatest degrees of movements of these elements in and out of the open system produced aplite and pegmatite in the center of the dike where the maximum angle of deflection occurred in the S-shaped flexure. From a distance, the dike appears to transect the diorite as a single continuous body, but in reality, the aplite and pegmatite in the dike represent connections between multiple fillings of low-pressure sites in the flexed rocks (Fig. 5).

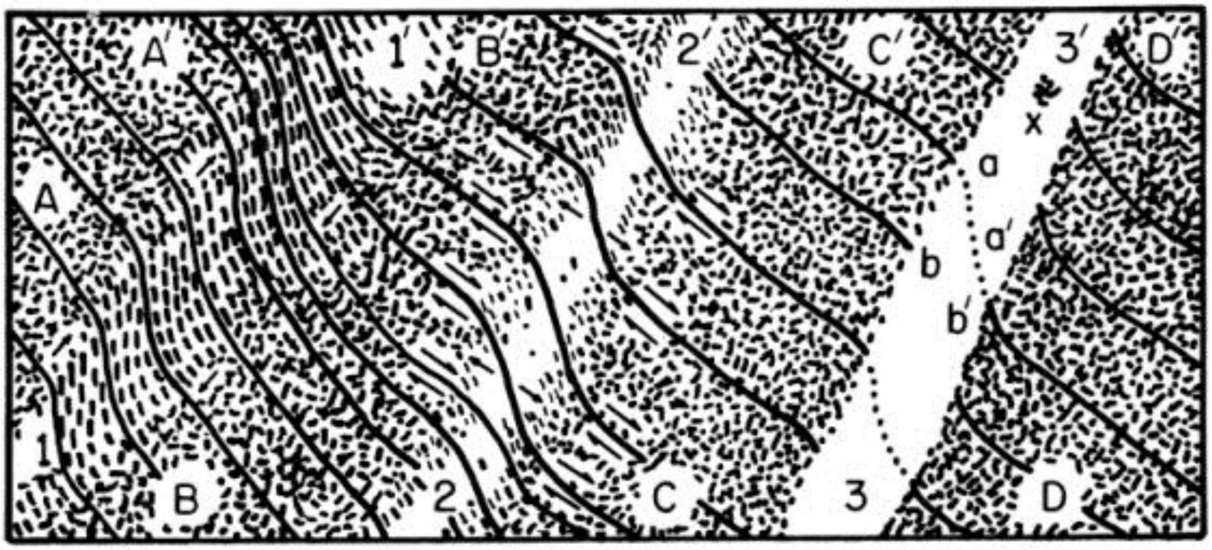


**Fig. 5.** Diagram showing theoretical stages in the formation of aplite and pegmatite dikes that replace diorite-gabbro wall rock. Areas between A-A', B-B', C-C', and D-D' represent the original massive diorite-gabbro with randomly oriented crystals. Area between 1-1' represents flexed rock in which shearing and cataclasis have oriented the crystals into parallel or subparallel alignment. Here the ferromagnesian silicates are partially replaced by quartz. Area between 2-2' shows differential movements parallel to foliation, which produce relatively low-pressure sites into which silica can move to replace the ferromagnesian silicates by quartz and into which K can move to replace zoned plagioclase to form microcline, myrmekite, and unzoned plagioclase. Migmatite can occur on either side of the 'dike,' but a central zone, where replacement is complete, is aplite or pegmatite. Remnant dark minerals show traces of the former flexed foliation. Area between 3-3' shows an aplite-pegmatite dike cutting across massive diorite-gabbro wall rock. A faint foliation is truncated by the granitic dike; layer b-b' appears to match up, however, a-a' actually connects equivalent layers. Island x is a remnant block of unsheared massive diorite-gabbro which remained as an enclave in the dike.

In other dikes in the northern part of the diorite-gabbro (Fig. 2), shearing and cataclasis allowed similar movements of major- and trace-elements to produce myrmekite-bearing granitic rocks, but zones 1 and 2 may be missing or narrow so that relatively sharp contacts exist between the granitic dikes and the diorite (or gabbro) wall rocks. In these places, foliated layers in the S-shaped structures have been stretched and broken, producing shear zones in which the fractured rocks have been thoroughly replaced and recrystallized.

## Chemical changes, leading to the formation of the Rb-Sr errorchrons

Chemical changes accompany the mineralogical changes that occur in zones 0-3 (Fig. 4). See Tables 1, 2, and 3 and Fig. 6 and Fig. 7. The chemical data are for the parent wall-rock diorite-gabbro (samples 12-16) and for diorite, transition rocks, migmatite, and aplite for four different dikes (samples 33-38, 39-40, 41-42, and 43-44); see Fig. 8 for sample locations and Appendices A and C in Collins, 1988, for rock sample descriptions). For comparison, Fig. 6 also shows fields of data for other samples from the Kernville diorite-gabbro and from the granitic rocks of the Isabella pluton (Collins, 1988). The chemical data show that from the diorite (Fig. 4, zone 0) to the aplite-pegmatite in the dike (zone 3), there are progressive losses of oxides of Fe, Mg, Al, Ti, and Ca, and an increase in K as Na remains nearly constant (Fig. 6 and Fig. 7). However, in the earliest stages of replacement, K is subtracted from the diorite, causing a simultaneous enrichment in residual Na. Rb and Sr show parallel movements with K and Na.

| | Wall Rock | Trans. Rock | Migm. | Migm. | Aplite "dike" | Trans. Rock | Trans. Rock | Wall Rock | Aplite "dike" | Wall Rock | Aplite "dike" | Wall Rock |
|---|---|---|---|---|---|---|---|---|---|---|---|---|
| Wt. % | 33 | 34 | 35 | 36 | 37 | 38 | 39 | 40 | 41 | 42 | 43 | 44 |
| $SiO_2$ | 57.85 | 67.55 | 71.76 | 74.93 | 73.86 | 69.39 | 68.03 | 61.16 | 76.39 | 69.94 | 70.60 | 54.70 |
| $Al_2O_3$ | 18.19 | 15.96 | 13.16 | 13.56 | 14.57 | 15.40 | 16.71 | 16.93 | 13.72 | 15.20 | 15.10 | 17.45 |
| $Fe_2O_3$ | 7.76 | 3.37 | 1.40 | 1.53 | 1.48 | 3.22 | 3.31 | 7.06 | 0.55 | 3.10 | 3.34 | 9.05 |
| $TiO_2$ | 1.00 | 0.56 | 0.12 | 0.17 | 0.14 | 0.50 | 0.58 | 0.87 | 0.03 | 0.46 | 0.46 | 1.16 |
| MgO | 3.27 | 0.79 | 0.13 | 0.18 | 0.22 | 0.60 | 0.71 | 2.14 | 0.01 | 0.49 | 1.03 | 4.76 |
| CaO | 6.49 | 3.58 | 1.10 | 1.27 | 1.39 | 2.76 | 3.04 | 5.14 | 1.13 | 2.81 | 2.59 | 7.87 |
| $Na_2O$ | 3.24 | 4.67 | 2.74 | 3.22 | 3.13 | 3.58 | 3.63 | 3.67 | 2.88 | 4.71 | 2.95 | 2.92 |
| $K_2O$ | 1.89 | 1.17 | 5.39 | 5.04 | 5.87 | 3.81 | 3.54 | 2.10 | 4.96 | 1.65 | 4.01 | 1.58 |
| $P_2O_5$ | n.d. | n.d. | n.d. | n.d. | n.d. | n.d. | n.d. | n.d. | n.d. | n.d. | n.d. | n.d. |
| LOI | 0.75 | 0.89 | 4.84 | 0.50 | 0.41 | 1.09 | 1.22 | 0.95 | 0.61 | 0.62 | 0.57 | 1.03 |
| Total | 100.44 | 98.54 | 100.64 | 100.40 | 101.07 | 100.35 | 100.77 | 100.02 | 100.28 | 98.98 | 100.65 | 100.52 |
| ppm | | | | | | | | | | | | |
| Cu | 13 | 6 | 3 | 3 | 5 | 5 | 5 | 9 | 7 | 6 | 5 | 11 |
| Mo | 1 | 1 | 1 | 1 | 1 | 1 | 1 | 1 | 1 | 1 | 1 | 1 |
| Pb | 2 | 1 | 3 | 7 | 3 | 1 | 1 | 1 | 6 | 1 | 1 | 1 |
| Zn | 82 | 53 | 30 | 31 | 30 | 78 | 80 | 145 | 10 | 76 | 53 | 84 |
| Ni | 10 | 4 | 4 | 4 | 4 | 4 | 3 | 9 | 4 | 3 | 8 | 17 |
| Co | 16 | 6 | 2 | 2 | 2 | 3 | 4 | 10 | 2 | 3 | 6 | 16 |
| Mn | 450 | 190 | 185 | 250 | 222 | 262 | 298 | 770 | 50 | 275 | 480 | 590 |
| Ba | 820 | 1,200 | 580 | 1,160 | 1,100 | 1,740 | 1,420 | 520 | 1,260 | 340 | 540 | 480 |
| Ag | 0.1 | 0.1 | 0.1 | 0.1 | 0.1 | 0.1 | 0.1 | 0.1 | 0.1 | 0.1 | 0.1 | 0.1 |
| W | 1 | 1 | 1 | 1 | 1 | 1 | 1 | 1 | 1 | 1 | 1 | 1 |
| Sn | 1 | 1 | 2 | 1 | 1 | 1 | 1 | 1 | 1 | 1 | 1 | 1 |
| Rb* | 74.8 | 46.9 | 203.0 | 195.0 | 218.0 | 105.0 | 102.0 | 93.4 | 129.0 | 125.0 | 180.0 | 59.0 |
| Sr* | 498 | 683 | 198 | 243 | 249 | 569 | 579 | 445 | 265 | 406 | 242 | 511 |
| ppb | | | | | | | | | | | | |
| Hg | 50 | 40 | 30 | 30 | 20 | 30 | 40 | 30 | 40 | 40 | 20 | 30 |
| Au | 2 | 3 | <1 | 3 | 2 | 1 | 2 | 2 | <1 | 3 | 2 | 2 |

Analyses by Chemex Labs Ltd., except for Rb and Sr. LOI = loss on ignition; n.d. = not determined. * Analyst, R. Kistler.

**Table 1**. Chemical analyses of major and trace elements in the Kernville diorite wall rock, transition rocks, migmatite, and aplite dikes.

| Spec. No. | $\delta^{18}O$ | Rb ppm | Sr ppm | Rb/Sr (wt. ratio) | $^{87}Rb/^{86}Sr$ (atom ratio) | $^{87}Sr/^{86}Sr$ (atom ratio) |
|---|---|---|---|---|---|---|
| 33 | + 9.3 | 74.8 | 498.0 | 0.150 | 0.435 | 0.70813 ± 3 |
| 34 | +11.1 | 46.9 | 683.0 | 0.069 | 0.199 | 0.70827 ± 4 |
| 35 | +10.7 | 203.0 | 198.0 | 1.025 | 2.970 | 0.71134 ± 3 |
| 36 | +10.3 | 195.0 | 243.0 | 0.802 | 2.320 | 0.70951 ± 3 |
| 37 | +10.5 | 218.0 | 249.0 | 0.876 | 2.530 | 0.71104 ± 4 |
| 38 | +11.3 | 105.0 | 569.0 | 0.184 | 0.534 | 0.70887 ± 3 |
| 39 | +11.7 | 102.0 | 579.0 | 0.176 | 0.510 | 0.70848 ± 4 |
| 40 | +10.8 | 93.4 | 445.0 | 0.210 | 0.607 | 0.70857 ± 3 |
| 41 | +11.7 | 129.0 | 265.0 | 0.487 | 1.410 | 0.70937 ± 4 |
| 42 | +11.5 | 125.0 | 406.0 | 0.308 | 0.891 | 0.70886 ± 3 |
| 43 | +10.9 | 180.0 | 242.0 | 0.744 | 2.150 | 0.71044 ± 5 |
| 44 | +10.0 | 59.0 | 511.0 | 0.115 | 0.334 | 0.70776 ± 3 |

Rb and Sr by x-ray fluorescence; Rb/Sr ± 3.0%. Analyst, R. Kistler

$\delta^{18}O$ data, analyst, Sergio Hauser

**Table 2**. Delta $^{18}O$, Rb, and Sr analyses of diorite, transition rocks, and granitic aplite dikes in the Kernville pluton. Discussion of $\delta^{18}O$ values is omitted in the text; see Collins (1988).

| Spec. No. | $\delta^{18}O$ | Rb ppm | Sr ppm | Rb/Sr (wt. ratio) | $^{87}Rb/^{86}Sr$ (atom ratio) | $^{87}Sr/^{86}Sr$ (atom ratio) | $^{87}Sr/^{86}Sr$ (initial) |
|---|---|---|---|---|---|---|---|
| 1 | +10.9 | 67.5 | 445.0 | 0.152 | 0.439 | 0.72032 ± 5 | |
| 2 | +13.7 | 123.0 | 165.0 | 0.745 | 2.160 | 0.73827 ± 5 | |
| 3 | +11.0 | 195.0 | 470.0 | 0.415 | 1.200 | 0.70875 ± 4 | 0.70726 ± 9 |
| 4 | + 9.1 | 82.9 | 732.0 | 0.113 | 0.328 | 0.70713 ± 4 | 0.70663 ± 4 |
| 5 | + 9.1 | 107.0 | 615.0 | 0.174 | 0.503 | 0.70746 ± 3 | 0.70663 ± 4 |
| 6 | + 9.3 | 69.3 | 776.0 | 0.089 | 0.258 | 0.70706 ± 4 | 0.70663 ± 4 |
| 7 | +10.1 | 116.0 | 378.0 | 0.307 | 0.888 | 0.70805 ± 4 | 0.70663 ± 4 |
| 8 | +10.2 | 124.0 | 480.0 | 0.258 | 0.747 | 0.70813 ± 5 | 0.70726 ± 9 |
| 9 | +10.6 | 99.0 | 366.0 | 0.270 | 0.783 | 0.70854 ± 3 | 0.70723 ± 9 |
| 10 | +12.5 | 122.0 | 35.6 | 3.430 | 9.960 | 0.75232 ± 5 | |
| 11 | +10.6 | 195.0 | 29.6 | 6.590 | 19.100 | 0.73642 ± 4 | 0.70723 ± 9 |
| 12 | + 8.8 | 10.0 | 780.0 | 0.013 | 0.037 | 0.70681 ± 5 | 0.70675 ± 4 |
| 13 | + 9.8 | 13.5 | 623.0 | 0.022 | 0.063 | 0.70686 ± 4 | 0.70675 ± 4 |
| 14 | + 9.2 | 117.0 | 408.0 | 0.287 | 0.830 | 0.70814 ± 3 | 0.70675 ± 4 |
| 15 | + 8.9 | 110.0 | 407.0 | 0.270 | 0.782 | 0.70811 ± 4 | 0.70675 ± 4 |
| 16 | + 9.3 | 113.0 | 384.0 | 0.294 | 0.851 | 0.70770 ± 3 | |
| 17 | + 9.4 | 57.7 | 517.0 | 0.117 | 0.323 | 0.70768 ± 4 | 0.70719 ± 9 |
| 18 | +10.1 | 148.0 | 318.0 | 0.465 | 1.350 | 0.70925 ± 5 | 0.70719 ± 9 |
| 19 | + 9.4 | 71.6 | 459.0 | 0.156 | 0.451 | 0.70917 ± 4 | |
| 20 | + 9.3 | 57.7 | 471.0 | 0.123 | 0.354 | 0.70821 ± 3 | 0.70764 ± 9 |
| 21 | + 9.8 | 103.0 | 366.0 | 0.281 | 0.814 | 0.70908 ± 4 | 0.70764 ± 9 |
| 22 | + 9.9 | 99.5 | 306.0 | 0.325 | 0.941 | 0.70918 ± 5 | 0.70764 ± 9 |
| 23 | +10.6 | 171.0 | 392.0 | 0.436 | 1.260 | 0.70904 ± 3 | 0.70723 ± 9 |
| 24 | +12.2 | 91.2 | 521.0 | 0.175 | 0.506 | 0.70762 ± 5 | 0.70675 ± 4 |
| 25 | +11.3 | 133.0 | 28.9 | 4.600 | 13.340 | 0.73010 ± 5 | 0.70764 ± 9 |

Rb and Sr by x-ray fluorescence; Rb/Sr ± 3.0%. Analyst, R. Kistler
$\delta^{18}O$ data, analyst, Sergio Hauser

**Table 3**. Delta $^{18}O$, Rb, and Sr analyses of rocks in the Kernville and Isabella plutons. Discussion of $\delta^{18}O$ values is omitted in the text; see Collins (1988).

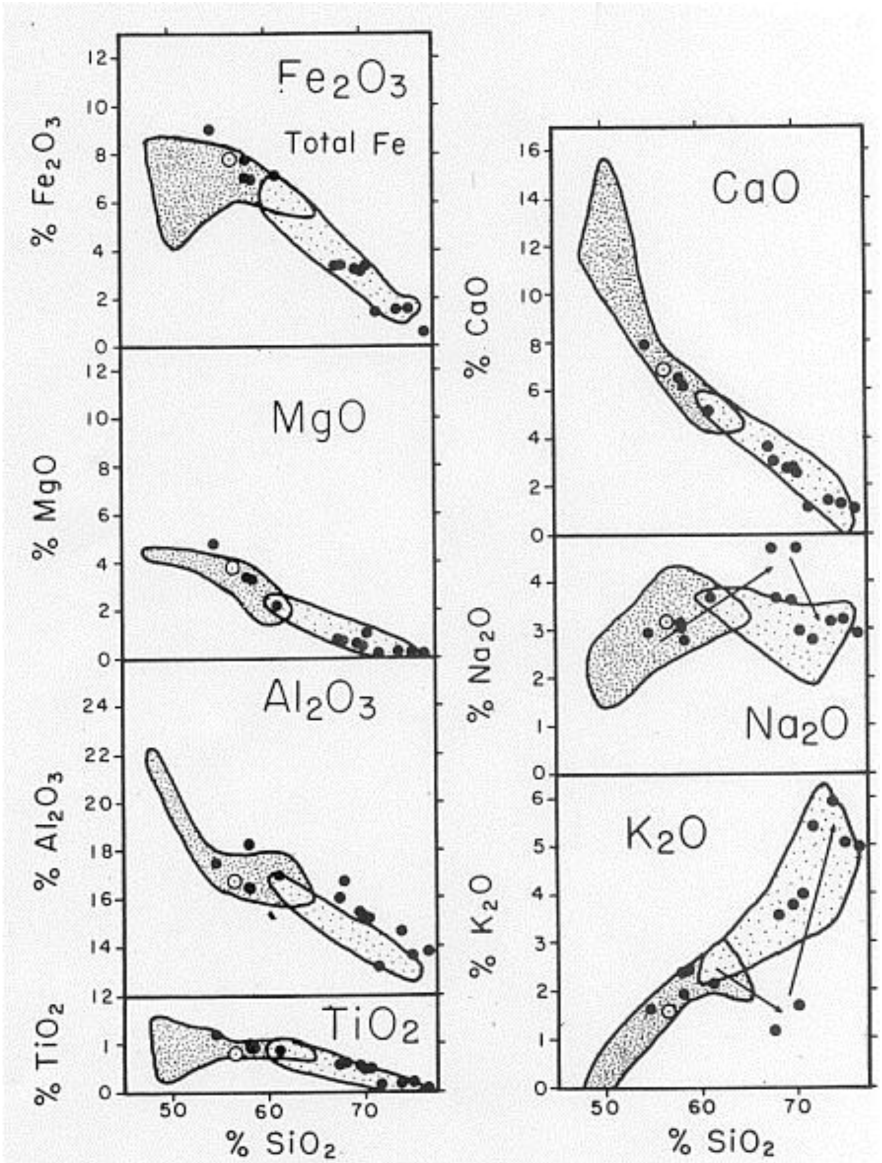


**Fig. 6.** Weight percentages of major oxides plotted against $\%SiO_2$ for samples nos. 13-16 and 33-44 (black dots), including diorite, transition rocks, and aplite dikes in diorite-gabbro wall rocks in the Kernville pluton. Open circle = sample no. 16 (diorite adjacent to the Isabella pluton). Outlined fields trace position of diorite-gabbro wall rocks (dark-shaded field) and granitic rocks of the Isabella pluton (light-shaded field) shown in Fig. 24 in Collins (1988). Arrows indicate localized loss of $K_2O$ and proportional enrichment in $Na_2O$; see also Fig. 24 in Collins (1988). The loss of $K_2O$ suggests that some of the K that forms K-feldspar (microcline) in the recrystallized granitic rocks is derived partly from the biotite in the modified diorite wall rock. More K must come in from deeper sources to account for all K-feldspar, and some Si must come in to explain the volumes of quartz.

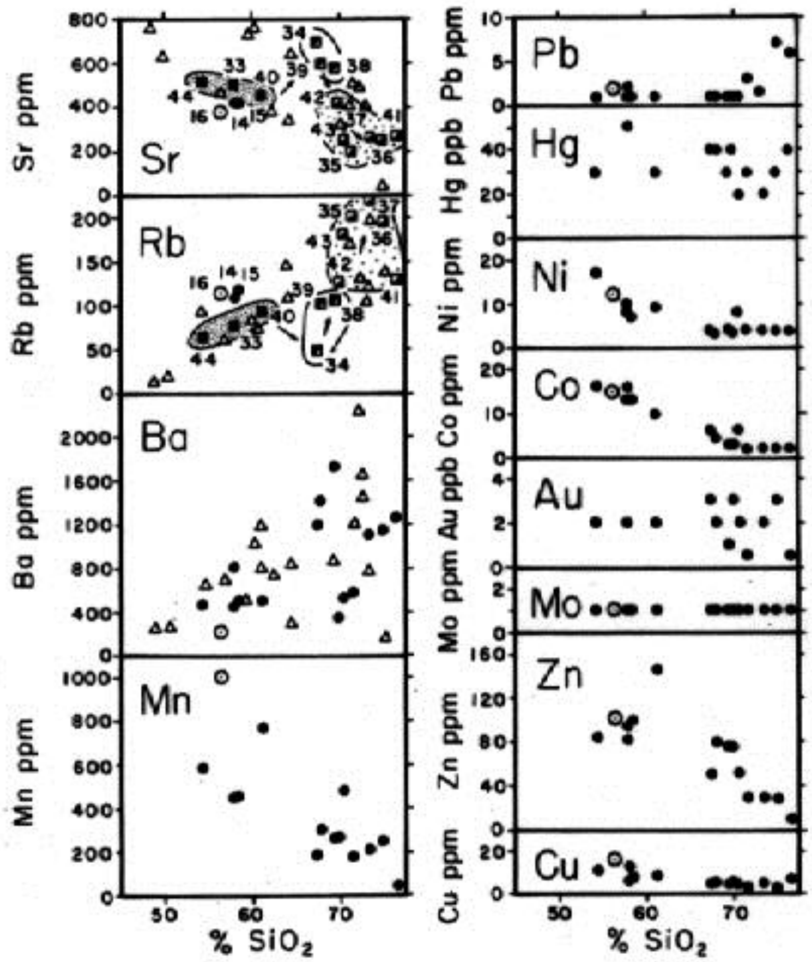


**Fig. 7.** Parts per million Sr, Rb, Ba, Mn, Pb, Ni, Co, Mo, Zn, and Cu and parts per billion Hg and Au plotted against weight % $SiO_2$ for rock samples in the diorite-gabbro wall rock (solid black circles). For diagrams that include Sr and Rb data, the sample numbers have been differently designated and separated into three fields. These include diorite wall rocks from Table VI in Collins (1988). Solid circles indicate diorite , sample nos. 14 and 15; open circle indicates sample no. 16 (foliated diorite adjacent to the Isabella pluton). Black squares indicate diorite (nos. 33, 40, and 44); squares shaded in the northwest half indicate transition rocks (nos. 34, 38, and 39); and squares shaded in the southeast half indicate migmatized diorite and aplite dike samples (nos. 35, 36, 37, 41, 42, and 43). For diagrams that include Sr, Rb, and Ba, the open triangles represent other diorite-gabbro wall rock samples shown in Tables VI and VII in Collins (1988). Arrows in the diagrams showing Sr and Rb data indicate trend of subtraction of Rb and enrichment in Sr during shearing and recrystallization in the diorite-gabbro followed by enrichment of Rb and subtraction of Sr during the subsequent replacement of these rocks to produce the granitic rocks in the aplite-pegmatite dike.

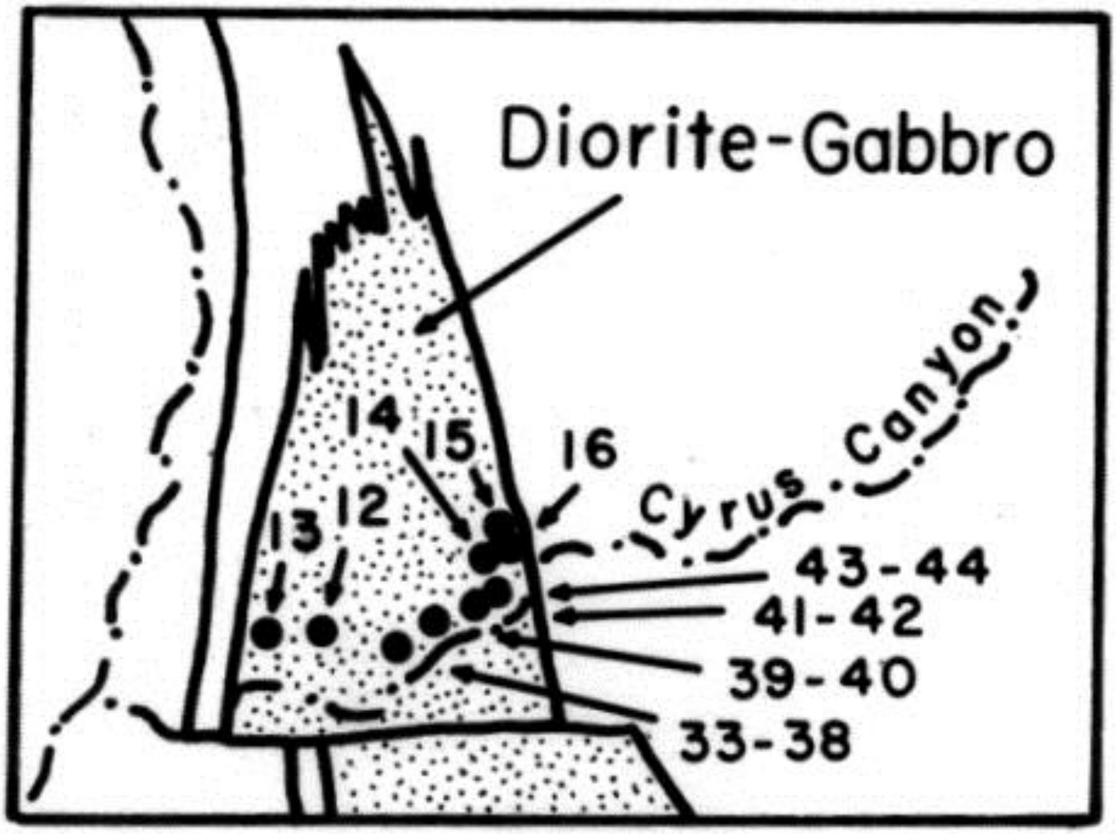


**Fig. 8.** Location map of chemically analyzed samples listed in Tables 1, 2, and 3.

## The resulting Rb-Sr errorchron

All of the differential movements of major and trace elements in an open system mean that Rb and Sr isotopes are also affected differentially. If data for these isotopes are plotted on a diagram with $^{87}Sr/^{86}Sr$ values versus $^{87}Rb/^{86}Sr$ values, a large scatter of data points occurs (Fig. 9). Because the scattered points do not fall on or nearly on a straight isochron line, indicating a particular evolutionary age date, only an errorchron can be drawn. Although the errorchron does not necessarily indicate an accurate time, the scatter of Rb and Sr isotopic data associated with it provides significant information about what has happened in the rock from which these data were obtained. To understand what has affected the Rb-Sr systematics requires attention to chemical and mineralogical changes that occurred in the rocks.

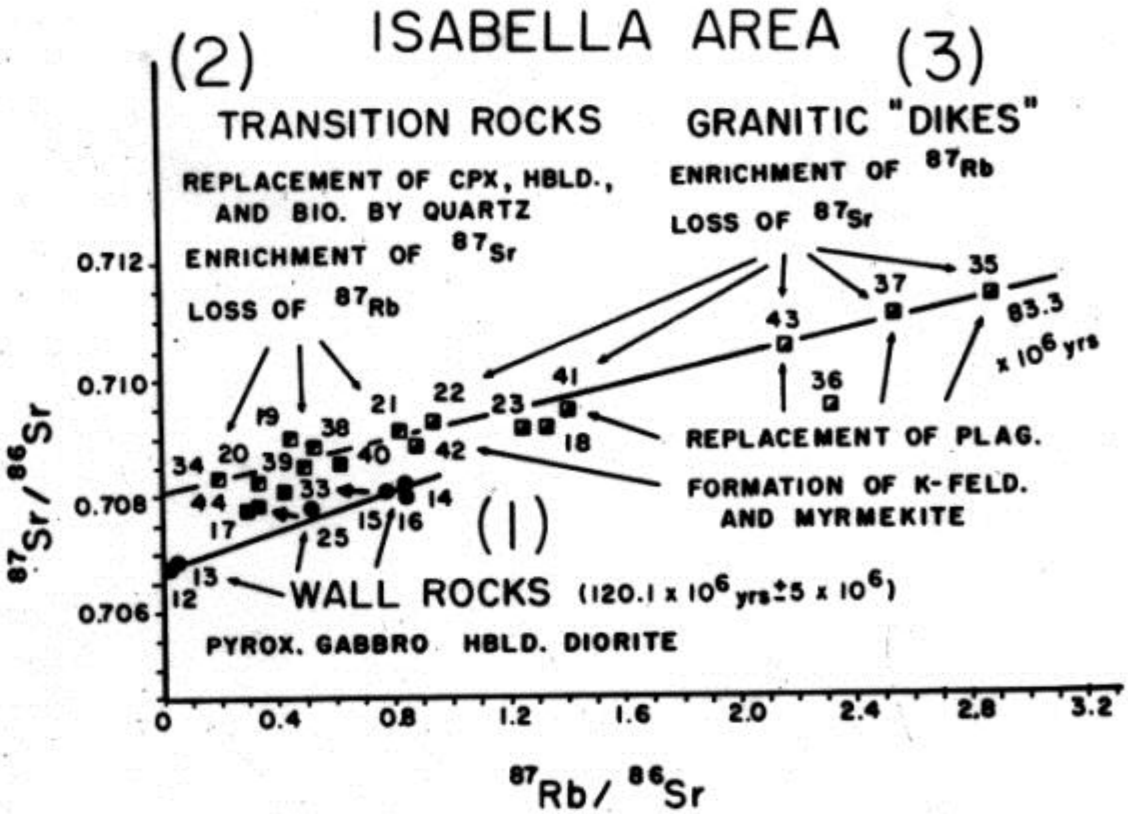


**Fig. 9.** Isochron plot of (1) biotite-hornblende diorite and hornblende-pyroxene gabbro wall rocks, (2) transition rocks, and (3) granitic aplite dikes in the Kernville pluton; see text. The other samples give an average date of 83.3 million years old. Solid circles indicate diorite, sample nos. 14 and 15; open circle indicates sample no. 16 (foliated diorite adjacent to the Isabella pluton). Black squares indicate modified diorite (nos. 33, 40, and 44); squares shaded in the northwest half indicate transition rocks (nos. 34, 38, and 39); and squares shaded in the southeast half indicate migmatized diorite and aplite dike samples in which plagioclase is replaced by microcline and myrmekite (nos. 35, 36, 37, 41, 42, and 43). Numbers adjacent to symbols refer to sample numbers in Tables 1, 2, and 3, and Tables VI and VII in Collins (1988).

**Factors in Rb-Sr systematics that contribute to formation of a Rb-Sr errorchron**

There are a number of factors to consider when the Rb-Sr systematics in the parent and modified diorite is examined.

(1) Because Rb has the same chemistry as K and because Sr has the same chemistry as Ca, it is logical that both K and Rb will move together in hydrous fluids as will Sr and Ca.

(2) Both K and Rb preferentially occur in K-feldspar or biotite, whereas common Sr and Ca are found mostly in plagioclase.

(3) In diorite devoid of K-feldspar, Rb, including radiogenic $^{87}$Rb, is concentrated in biotite.

(4) Because $^{87}$Rb decays to $^{87}$Sr, biotite contains relatively abundant $^{87}$Sr in comparison to its meager content of common Sr and may contain most of the radiogenic $^{87}$Sr in the rock.

(5) In earliest stages of the open system that was created in the deformed Kernville diorite, total Sr is enriched in the rocks, indicating that common Sr tends to remain behind with Na in altered plagioclase crystals while some Ca is being removed from plagioclase and the system (Fig. 6 and Fig. 7). Because Sr has a larger ionic size than Ca and is closer to the ionic size of Na, this may explain why Sr tends not to go out with Ca. At the low temperatures that occur in the open system, a more sodic plagioclase is more stable than a more calcic plagioclase.

(6) Later, common Sr gradually leaves the system as K replaces Na, Ca, and Sr in microfractured plagioclase to form K-feldspar. Thus, in late stages the total Sr in the altered rock progressively becomes less (Fig. 7). Again, at the low temperature, K-feldspar is the more stable mineral than plagioclase.

(7) Moving fluids, however, do not distinguish between common Sr and radiogenic $^{87}$Sr, and, therefore, both radiogenic and non-radiogenic Sr will move simultaneously out of the system when both Ca and Sr are extracted.

(8) K, Rb (including $^{87}$Rb), and $^{87}$Sr are released from biotite when the biotite is replaced by quartz.

(9) K and Rb (including $^{87}$Rb) move into newly formed K-feldspar, and, therefore, Rb tends to be enriched and remain in a rock, whereas much common Sr and $^{87}$Sr will eventually leave the open system. Nevertheless, the $^{87}$Sr/$^{86}$Sr ratios will have been increased in the modified rock because some $^{87}$Sr still remains in residual biotite that has not yet been replaced by quartz while large amounts of common Sr and trace amounts of $^{87}$Sr are being displaced by K in plagioclase.

With these nine observations in mind, the movements of Rb, $^{87}Rb$, common Sr, and $^{87}Sr$ can be traced on Fig. 9 from the parent diorite (Fig. 4, zone 0) through the transition rocks (zone 1) where the diorite is first being modified, and then progressively through rocks showing greater degrees of modification to zone 3, where the greatest degree of modification occurs. Of course, the plotted data on Fig. 9 represent the present time after decay of $^{87}Rb$ to form additional $^{87}Sr$, but the trends of the original changes are still the same.

**The sequential movements of Rb and Sr isotopes and other elements**

As indicated by the chemical analyses plotted in Fig. 6 and Fig. 7, the following show the sequential isotopic and elemental changes that occur as diorite is converted to aplite-pegmatite.

(1) The unaltered original diorite is represented by samples 14, 15, and 16 (Table 3), and the starting isotopic data for these samples are plotted at the upper end of the isochron indicating a 120.1 million-year-old age. These samples are labeled as wall rocks for the aplite-pegmatite dikes as well as being the wall rocks for the Isabella pluton (Fig. 1).

(2) In the first stages of modification, biotite begins to be replaced by quartz and loses K, $^{87}Rb$, and $^{87}Sr$, as altered plagioclase begins to lose Ca. However, Na remains behind in the plagioclase as does common Sr. The released K and $^{87}Rb$ are carried away toward the structural low-pressure sites (Fig. 5) in zone 3, but $^{87}Sr$ tends to stay behind and move into the altered plagioclase crystals with residual Na. The combination of these relative movements means that the $^{87}Rb/^{87}Sr$ values in the modified diorite samples decrease greatly as the $^{87}Sr/^{86}Sr$ values increase slightly. These changes are shown by arrows, pointing in the direction of data points that are plotted as solid squares on Fig. 9 (samples 33, 40, and 44).

(3) Farther along in zone 1, biotite continues to be replaced by quartz so that more K, $^{87}Rb$, and $^{87}Sr$ are released, but some K and $^{87}Rb$ begin to move into altered plagioclase crystals to form K-feldspar while some $^{87}Sr$ continues to move into other altered plagioclase grains, causing the $^{87}Sr/^{86}Sr$ values to rise still further. These relative movements of elements cause the $^{87}Rb/^{86}Sr$ values to reach a minimum at some point and then rise as $^{87}Rb$ begins to concentrate in the newly formed K-feldspar and as some Ca and Sr in the microfractured plagioclase crystals are displaced by K and begin to leave the system. Rocks representing this stage have low $^{87}Rb/^{86}Sr$ values and are plotted higher on Fig. 9 as squares shaded in the northwest half (samples 34, 38, and 39).

(4) In final stages, as K and $^{87}Rb$ replace many altered plagioclase crystals to form more K-feldspar, even more Ca and Sr are displaced by the introduced K and $^{87}Rb$ and carried out of the system. The combination of these elemental changes causes the $^{87}Rb/^{86}Sr$ values to increase rapidly. The result is represented by aplite-pegmatite samples 35, 36, 37, 41, 42, and 43 that are plotted in the upper middle and upper right on Fig 9 as squares shaded in the southeast half.

All of these relative movements of the different elements and isotopes show how the rock adjusts its Rb and Sr systematics so that the initial $^{87}Sr/^{86}Sr$ ratio is reset to a higher value for the granitic rocks than occurs in the original diorite-gabbro isochron. Although no accurate determination of age is possible, if the data points are chosen for samples 41, 43, 37, and 35 that exhibit higher $^{87}Rb/^{86}Sr$ values, and if an initial $^{87}Sr/^{86}Sr$ ratio is selected for these values, an errorchron can be drawn whose slope indicates an average age of 83 million years old (Fig. 9). Saleeby reported (written communication, 2004) that his best number for the age of the maximum shearing along the Proto-Kern Canyon-Sierra Crest Fault Zone is about 85 million years ago and that shearing continued but waned until 80 million years ago, so perhaps the 83 million-year-old age is related to this shearing (Busby-Spera and Saleeby, 1990).

## Conclusion

The changes in fabric, mineralogy, structure, and chemistry that occur in an open system in deformed diorite in the Kernville pluton provide data that show how a Rb-Sr errorchron is produced. Differential movements of major and trace elements are accompanied also by differential movements of both Rb and Sr isotopes which cause a large scatter of data on an isochron plot. The movements of all these elements and isotopes contrast with the assumption often made that only Sr moves where an errorchron is produced. On that basis, Rb and Sr isotopic data that plot off a straight-line isochron for rocks that have been analyzed in other terranes are significant and should not be discarded or ignored because such data may be a clue that these rocks have been strongly modified mineralogically and chemically.

## Application to the Kernville gabbro

Although similar chemical and isotopic studies have not been done for aplite-pegmatite dikes adjacent to deformed pyroxene-hornblende gabbro wall rocks in the western part of the diorite-gabbro mass (Fig. 2, samples 12 and 13), some mineralogical studies have been made (Collins, 1988). Mineralogical changes that occur in the replaced gabbroic rocks are generally parallel to that which occurs in replaced diorite except that the resulting replacement granitic dikes in gabbro tend to be richer in quartz, contain less K-feldspar, and have myrmekite with coarser quartz vermicules. These differences result probably because the parent unmodified gabbro contains little biotite that could be a source of some of the K and has primary plagioclase with higher Ca content ($An_{40-70}$). These differences in dike compositions would not be expected if the granitic dikes were formed from magma of uniform composition which was injected simultaneously into cracks in both diorite and gabbro from the Isabella pluton. Moreover, the outer, westernmost, 500-m-wide granitic rock that extends along the western margin of the Kernville pluton and which appears to be an extension of the Isabella pluton (Fig. 1 and Fig. 2) is likely rock that lies within the Proto-Kern Canyon-Sierra Crest Fault Zone (Saleeby, 2003) in which the former gabbro has been repeatedly sheared, multiply replaced, and recrystallized as a fine-grained, quartz-rich, granitic aplite. The Rb-Sr systematics in this border rock should be thoroughly disrupted in the open system and produce even greater scatter in a Rb-Sr errorchron.

**Acknowledgements**

We wish to acknowledge the help of Robert Kistler for providing a Rb-Sr age of the Kernville pluton and Jason Saleeby for giving an age range for the Proto-Kern Canyon-Sierra Crest Fault Zone.

**References**

Busby-Spera, C J., and Saleeby, J. B., 1990, Intra-arc strike-slip fault exposed at batholithic levels in the southern Sierra Nevada, California: Geology, v. 18, n. 3, p. 255-259.

Collins, L. G., 1988, *Hydrothermal differentiation and myrmekite - A clue to many geological puzzles*: Athens, Theophrastus Publications, 387 p.

Collins, L. G., 1989, Origin of the Isabella Pluton and its enclaves: California Geology, v. 42, n. 3, March, p. 53-59.

Elan, R., 1985, High grade metamorphism at the Lake Isabella north shore roof pendant, southern Sierra Nevada, California: Master's thesis, University of Southern California, Los Angeles, 202 p.

Hunt, C. W., Collins, L. G., and Skobelin, E. A., 1992, *Expanding Geospheres, Energy And Mass Transfers From Earth's Interior*: Calgary, Polar Publishing Company, 421 p.

Miller, W. J., 1931, Geologic sections across the southern Sierra Nevada of California: University of California Publications, Bulletin of the Department of Geological Sciences, v. 20, n. 9, p. 331-360.

Miller, W. J., and Webb, R. W., 1940, Descriptive geology of the Kernville Quadrangle, California: California Journal of Mines and Geology, v. 36, no. 4, p. 343-378.

Saleeby, J., 2003, Segmentation of the Laramide Slab - evidence from the southern Sierra Nevada region: Geological Society of America Bulletin, v. 115, p. 655-668.